ARMA 18–806

Temporal borehole breakout evolution and its impact on stress estimation

Valley, B.
Center for Hydrogeology and Geothermics, University of Neuchâtel, Neuchâtel, Switzerland
Azzola, J. and Schmittbuhl, J.
École et Observatoire des Sciences de la Terre (EOST), Strasbourg, France
Genter, A.
ÉS géothermie, Schiltigheim, France

ABSTRACT: The estimation of the in-situ stress state is required for the design and execution of deep engineering operations related to Enhanced Geothermal System (EGS). Borehole failures, often referred as borehole breakouts, which are controlled by local stress concentration around the wellbore, are recognized being a useful indicator to assess in-situ stress conditions. However, breakouts evolve with time and this may affect our ability to use them for quantifying the stress state. We use a unique data set from the deep geothermal well of Rittershoffen GRT-1 in order to verify the hypothesis concerning wellbore breakout geometrical evolution. In GRT-1 wellbore, imaging has been acquired 4 days, 348 days and 946 days after drilling completion. Thermal, hydraulic and chemical stimulations have been performed between the first and the second image acquisition. Using this data set, we were able to describe in-situ the breakout evolution with time. We show increase in the extension of breakouts along the well. Contrary to the common assumptions, we also show that breakout widen, but within the limit of the accuracy of our analysis they do not deepen. The consequences of the breakout evolution for stress characterization are significant and add up to other important uncertainties in such analyses like the estimation of strength parameters.

1. INTRODUCTION

A large amount of energy is available at depth. This energy can be extracted by circulating fluids between boreholes through the hot rock mass, but this requires that sufficient permeability is present at depth. As permeability tends to decrease with depth (Manning and Ingebritsen 1999), it is necessary to target deep structures with locally higher permeability (e.g. fault zones) and/or to perform permeability enhancement operations. The later approach is referred as Enhanced Geothermal Systems (EGS). The principle underlying this technology consists of increasing the hydraulic performance of the reservoir through different types of stimulations so that commercially interesting flow rate can be achieved. The stimulations consist of high-pressure injection (hydraulic stimulation), cold water injection (thermal stimulation) or chemical injection (chemical stimulation). In the two first cases, the permeability increase is obtained by inducing a thermo-hydromechanical perturbation to the rock mass which reactivates existing structures or create new ones. The in-situ stress state is central to understand the response of the rock mass to injections and to design such operations.

Despite its importance, the in-situ stress state is always difficult to fully characterize, particularly in situations where the rock mass is accessed only by a few deep boreholes. In such cases, it is suggested to use borehole logging data and indication of borehole wall failure in order to give constraints on the in-situ stress state (Zoback et al. 2003; Schmitt et al. 2012). However, it is difficult to extract truly quantitative stress estimates from such analyses since the appropriate failure model for the borehole wall is poorly constrained and the mechanisms controlling the time failure evolution of the borehole wall are not well understood (e.g. creep effects, visco-plasticity, stress corrosion,…). Indeed, such analyses are typically performed on a single set of images acquired a few days after drilling completion when it is unclear if a new stable state was established and the observed geometry is final.

In this study, we specifically tackle the question of borehole evolution with time. We are using for this a unique borehole logging data set collected in the GRT-1 borehole at the Rittershoffen (France) geothermal project. In this project, well borehole imaging has been repeated three times and this allows investigating the temporal evolution of breakouts.

In this paper, we present first the project context followed by a description of the data acquired in the GRT-1 well. We explain what processing was performed on this data in order to produce comparable breakout geometrical descriptors. We use this generated information to highlight the evolution of breakout shape with time and we assess how this evolution influences our ability to characterize the stress state in a geothermal reservoir.

2. PROJECT CONTEXT AND DATA SET

The ECOGI Project is located near the village of Rittershoffen in North-Eastern France (Alsace, Fig. 1a). It is a EGS geothermal project initiated in 2011 and the first commercial project of a long-term strategy to develop geothermal energy in Alsace (Baujard et al. 2017). The doublet is drilled between Betschdorf and Rittershoffen, 6 km east of the well-known site of Soultz-sous-Forêts, in Northern Alsace (Genter et al. 2010). Although not located on the same local structure, the site of Rittershoffen presents similarities with the site of Soultz-sous-Forêts. The conformation of the local horst and graben implies that the depth of the contact between the basement and the sedimentary cover is deeper at Rittershoffen than at Soultz-sous-Forêts. The stress state at Soultz has been extensively characterized

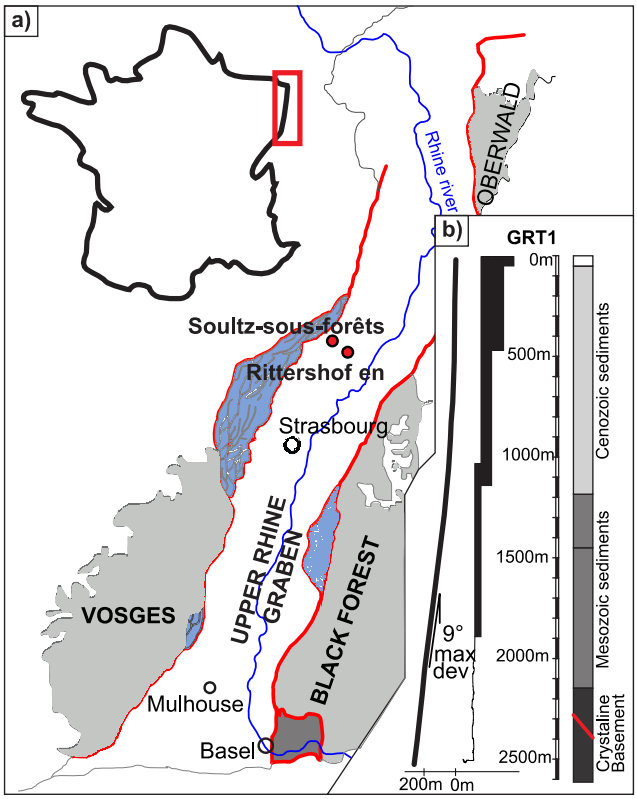

Fig. 1. a) geographic situation of the Rittershoffen project. b) simplified technical section of the GRT-1 borehole at Rittershoffen.

and indicates a transition in the stress regime from normal to strike-slip conditions (Valley 2007). The minimum horizontal principal stress (*Shmin*) is equal to about 0.54 the vertical stress and the maximum horizontal (*SHmax*) has a magnitude about equal to the vertical stress. Focal mechanisms study indicates a transition from normal dominated to strike-slip dominated mechanisms occurring with increasing depth (Cuenot et al. 2006). This transition takes place at depth of about 4 to 4.5 km. The Rittershoffen reservoir being shallower than this transition, it is likely in an essentially normal stress regime.

The first well of the Rittershoffen doublet, GRT-1, was completed in December 2013 and was drilled to a depth of 2580 m (MD, depth measured along hole) corresponding to a True Vertical depth of 2562 m TVD. The well penetrated the sediments / crystalline basement interface at a depth of 2212m MD and target a local fault structure (Duringer 2013). The 8" 1/2 diameter open-hole section of the well starts at 1922 m MD. The borehole is almost vertical with a maximum deviation of 9° only (Fig. 1b).

2.1. GRT-1 well characteristics and history

The first hydraulic testing showed an insufficient injectivity of the production well GRT-1. A major permeable structure controlling two third of the flow is intersected at 2368m MD (Baujard et al. 2017). The hydraulic connectivity between the well and the fracture network needed to be increased through a multi-step reservoir development strategy (Baujard et al. 2017), including first a thermal stimulation of the well in April 2013. Cold fluid (12°C) was injected at maximum rate of 25 l/s resulting in a maximum wellhead pressure of 2.8 MPa. A total volume of 4230 m^3 were injected. It was followed by a chemical stimulation of the well in June 2013. Using open hole packers, environmentally friendly acids, specifically developed based drilling cuttings mineralogy, were injected in specific zones. Finally, a hydraulic stimulation of the well was performed in June 2013. During this moderate volume injection, 3244 m^3 were injected in the open hole during 11h, with stepwise flowrates from 10L/s to 80L/s (Teza et al. 2013). The injectivity was improved fivefold due to this thermal, chemical and hydraulic (TCH) stimulation. Induced seismicity during and after shut-in has been monitored using a surface network of 18 stations. High resolution locations of the events evidence a large scale en-échelon structure of the targeted fault and suggest a triggering mechanism driven by aseismic slip (Lengliné et al. 2017).

2.2. GRT-1 borehole imaging data

Several extensive logging programs accompanied the drilling of well GRT-1. One was conducted in the open-hole section of GRT1, few days after drilling, in December 2012. It included especially acoustic

televiewer log. This is with this data type that we analyzed borehole failure. Two other borehole imaging logging campaign were conducted in GRT-1 in December 2013 after stimulation of the well and in June 2015.

A certain number of artefacts can deteriorate the quality of acoustic image data (Lofts and Bourke 1999). The images acquired in Rittershoffen suffer from some of these limitations. The quality of the image depends of the tool specification, the acquisition parameters and logging conditions. All acoustic images at Rittershoffen were acquired by Schlumberger with their UBI (Ultrasonic Borehole Imager) product. The tool and acquisition parameters were similar between each log, but not identical. For example, the GRT1 log in 2013 was acquired using a smaller acquisition head (see transducer diameter in Table 1). The acquisition resolution was the same for every log, i.e. 2° azimuthal resolution and 1 cm depth sampling step.

The 2012 log in GRT1 provides the best quality image of the entire suite. The image suffer in some limited sections of signal loss artefacts (Lofts and Bourke 1999), most commonly related to the presence of breakouts or major fracture zones.

The 2013 log in GRT1 is of comparable quality than the 2012 log and suffers also of some limited signal loss artefacts. The major issue with the GRT1-2013 log is that the orientation module was not included in the tool string and thus the image cannot be oriented with magnetometer data as it is usually done for this type of data.

The 2015 log in GRT1 generally suffers from more signal loss issues, not only in area with major fracture zones and breakouts. In the lower part of the log, wood grain artefact (Lofts and Bourke 1999) is also observable. This is particularly developed below 2431 m MD.

3. WELL BORE IMAGE PROCESSING AND BOREHOLE FAILURE DETERMINATION

3.1. Borehole image pre-processing

Prior to the analysis of failure, a suite of image preprocessing is required. This includes the following steps:

- **(i)** Transit time was converted to radius using the fluid velocity recorded during the probe trip down the borehole;
- **(ii)** Images were filtered to reduce noise;
- **(iii)** Digital image correlation was applied across the successive logs in order to correct the image misalignment both in azimuth and depth.

Table 1. Acquisition parameters of UBI logs in the GRT-1 borehole

Acquisition Date	Stimulation	Logging range [m; MD]	Transducer diameter [inch]
30-Dec-2012	4 days after drilling completion	1913.00 - 2568.00	4.9684
9-Dec-2013	After THC stimulation	1912.00-2531.16	2.9724
30-Jul-2015	No additional stimulation performed	1910.96-2499.9	4.9684

The computation of borehole radius was done using the borehole fluid velocity recorded during the trip downhole of the UBI probe and applying the standard formula from Luthi (2001):

$$r = \frac{t_{twt} \cdot v_m}{2} + d \quad (1)$$

with t_{twt} the two-way travel time, v_m the acoustic wave velocity in the drilling mud, and d the logging tool radius.

The image is filtered using a selective despiking algorithm implemented in WellCad™ using a cut-off high level (75%) and a cut-off low level (25%) in a 3x3 pixels window. These processes intend to remove spikes by replacing the radius value by the cut-off value if the data value exceeds the cut-off high or low level, the considered value is replaced.

Finally, digital image correlation was used to insure proper alignment of the images. This was required for the GRT1 2013 image because as mentioned above this image was not oriented with a magnetometer / accelerometer tool. The process was also applied to the 2015 GRT1 data to facilitate comparison across the entire GRT1 imaging log suite.

The image alignment was evaluated using two dimensional discrete cross-correlation, computed in successive thumbnails centered at position *(X,Y)* and defined along the images to be aligned. For each thumbnails pair, cross-correlation function is a measure of the similarity between the thumbnail taken in the reference image – i.e. the 2012 image in our case – with the thumbnail of the image to compare with - i.e. taken in the 2013 or 2015 image in our case – when it is shifted by a given displacement vector (*dX, dY*). The two dimensional cross-correlation function is an operator acting on two intensity functions *s(X,Y)* and *r(X,Y),* defined as a norm of the color levels at each position of each thumbnail. C_{sr} is defined at a position *(X,Y)* and for a shift *(dX, dY)* by:

$$C_{sr}(dX, dY) = s(X,Y) \otimes r(X,Y)$$
$$= \iint_{-\infty}^{+\infty} s(X,Y) r * (X - dX, Y - dY) dX dY \quad (2)$$

The position with the highest cross correlation correspond to the best aligned image. For our study we used a correlation box of size 180 pixels * 20 pixels. This horizontal configuration is appropriate to identify principally the azimuthal offset while it is less sensitive to the depth mismatch. We investigated offset up to 180 pixels horizontally corresponding for our 2° resolution to a complete 360° rotation. We considered vertical offset of ±10 pixels corresponding to offsets of ± 10cm. This correlation process allows to align finely the successive images and thus to study the borehole shape evolution with time.

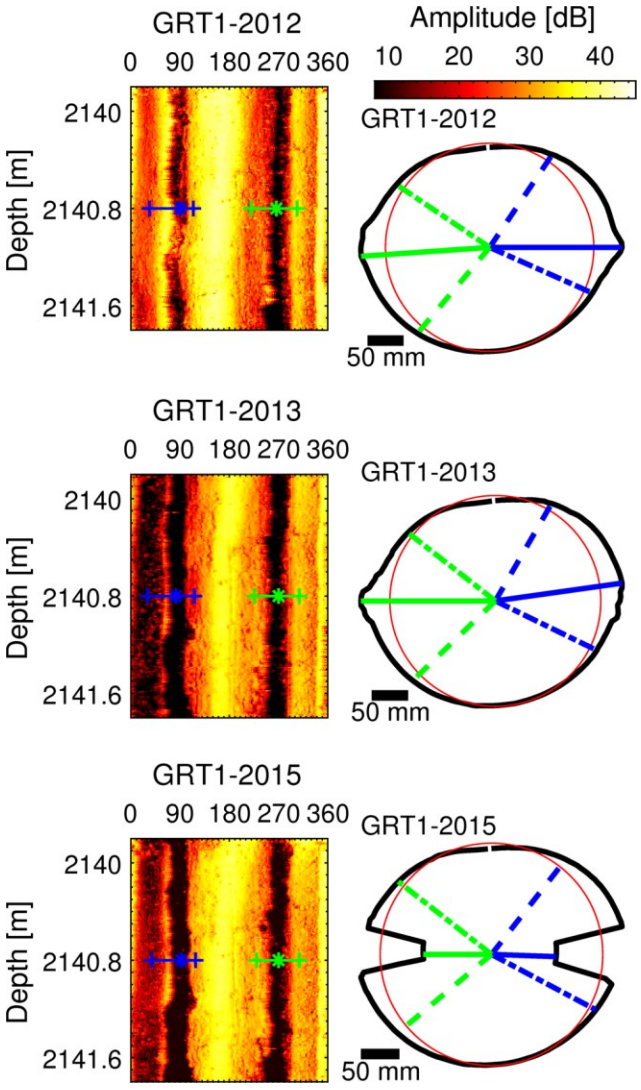

Fig 2. Example of breakout geometry determination. Left: amplitude images for GRT1 at 2140.8 m for the logs from 2012, 2013 and 2015. Right: wellbore section at 2140.8 m computed from the transit time image from the 2012, 2013 and 2015 logs respectively. The breakout extends are determined on the wellbore section and are present on the figures in blue and green.

3.2. Determination of borehole failure

The breakouts have been determined through a visual analysis of borehole sections computed every 20 cm from 1926 to 2568 m MD. The borehole sections are computed by stacking (averaging using the median) the data collected every 1 cm over 20 cm borehole interval (no overlap between two successive sections). The median is used because it is less sensitive to extreme values (resulting for example from noise) than the mean. In addition, the actual borehole center is determined by adjusting a best fitting ellipse to the borehole section.

For each section presenting the characteristic elongated shape due to stress induced failure, the azimuthal position of the edges and the center of each breakout limb are determined by visual inspection. Examples of such determination are given in Fig. 2. This determination is performed on wellbore sections generated from the transit time data. The breakout edges are defined as the location where the wellbore section departs from a circular section. As can be seen in Fig. 2, this typically spans an azimuthal range much broader than the low amplitude reflections visible as dark bands on the amplitude images. The positions of the breakout edges are not easy to determine in a systematic and indisputable manner and a significant uncertainty is associated with these measurements. Related to this issue, it is not possible to determine on the images what azimuthal range of the wellbore is enlarged by purely stress redistribution processes and what part is enlarged subsequently by the effects of drill string wear. In order to mitigate these limitations and enable comparisons between the three successive logs acquired in GRT1, breakouts measurements were performed on all three images concomitantly and consistently. We controlled for example that within a tolerance dictated by the uncertainties of the measurements, breakout width can only remain identical or increase, but not decrease between successive logs. From this record two breakout parameters are computed: (1) the breakout width, i.e. the angular opening of the breakout limbs and (2) the breakout depth, i.e. the larger well radius reach in the breakout limb center.

Drilling induced tension fractures (DITFs) are also identified on the GRT-1 borehole images. Azimuth of the DITFs was measured every 20 cm.

4. ANALYSES OF TEMPORAL BOREHOLE FAILURE EVOLUTION

Stress estimates derived from breakout shape analysis typically rely on a single borehole image data set. From this snapshot in time stresses are estimated while information on the evolution of breakout shape in time is not available. At Rittershoffen, three successive image logs interestingly allow the study of this evolution. Here,

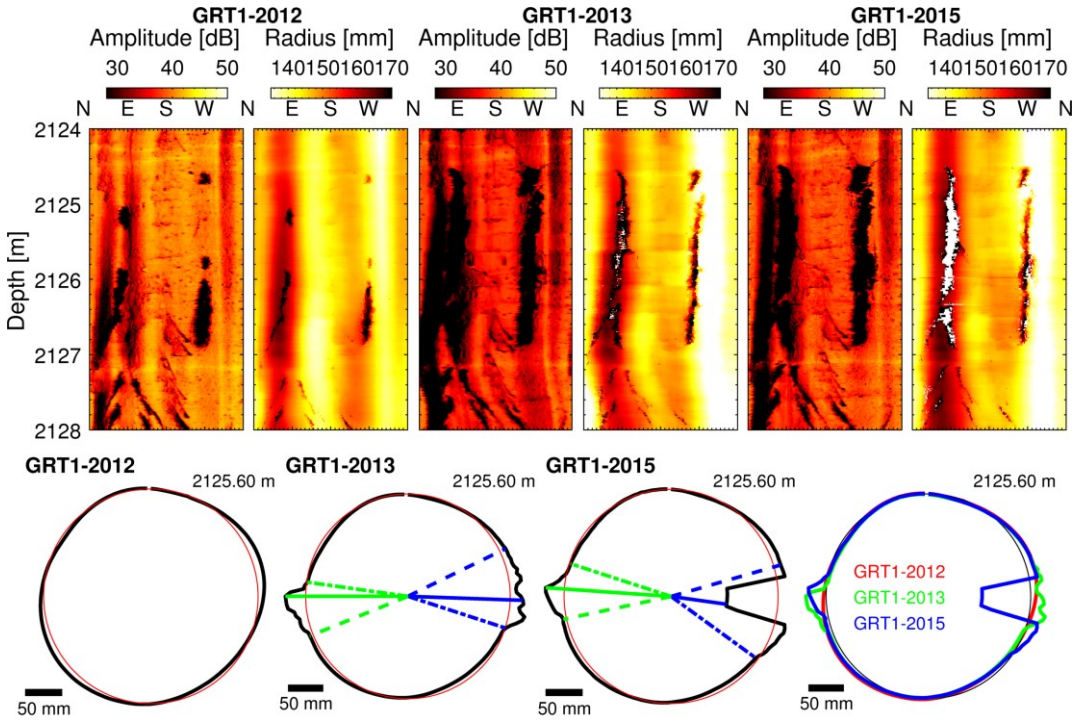

Fig. 3. Examples of breakout shape evolution between the three successive images collected in GRT1. At 2125.6 m there is no clear breakout in 2012, but breakout develops along the well and are visible in 2013 and 2015. Note also that due to signal loss artefact, the depth of failure on the eastern limb of the breakout is impossible to assess on the 2015 image.

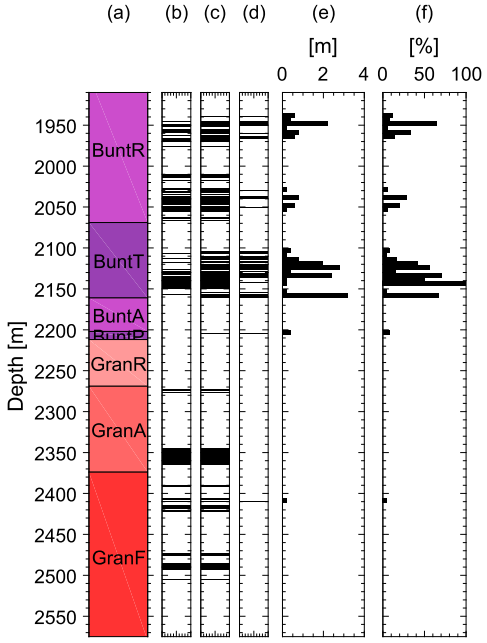

Fig. 4. Development of breakouts along GRT1 borehole between 2012 and 2013. a) Simplified lithologies along GRT1 borehole. Label with Bunt are mostly Triassic sandstones while labels with GRAN are crystalline basement with various level of weathering. b) Breakouts position in GRT1 in 2013. c) Breakouts positions in GRT1 in 2013. d) Intervals where breakouts are present in 2013 but not in 2012. e) Breakout length increase in [m] between 2012 and 2013 in 5 m bins. f) fraction in [%] of wellbore length that was free of breakout in 2012 that is presenting breakout on the 2013 image, computed in 5 m bins.

temporal evolution of the breakout width and depth is analyzed to characterize the temporal failure evolution of the borehole.

The common hypothesis concerning borehole breakouts evolution is that their width remains stable and is controlled by the stress state around the well at the initial rupture time (Zoback et al. 2003). Progressive failure is supposed to lead however to breakouts deepening until a stable profile is reached.

An example of comparison of breakout shape is presented in Fig. 3. The images in 2012, 2013 and 2015 show a clear breakout at a depth of about 2126 m in sandstone of the Triassic. The breakouts can show three types of evolution: 1) they can develop along the well; 2) they can widen; and 3) they can deepen. Fig. 3 shows a section of GRT-1 at around 2125m where those various processes are clearly depicted. At 2125.6 m failure did not occur in 2012 while breakouts are visible in 2013 and 2015. A superposition of the 2013/2015 borehole section shows no change in breakout shape for the west limb while a slight widening is visible on the east limb. Possible deepening of the east limb is occulted by time-out artefact.

The evolution of breakout occurrence along the well is presented in Fig. 4. Longitudinal failure development is quite common in the Buntsandstein while it is very limited in the basement granite. The evolution occurs exclusively between the 2012/2013 data set while no longitudinal extension occurs during 2013 and 2015. In

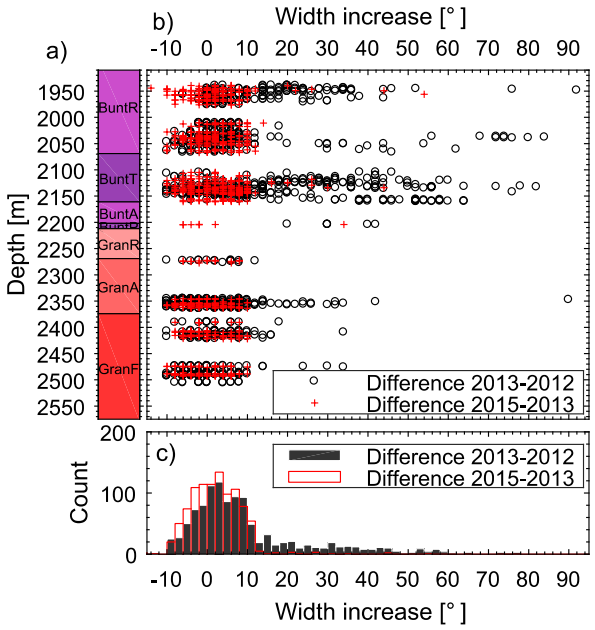

Fig. 5. evolution of breakout width in GRT-1 borehole. 1) Simplified lithologies along GRT1 borehole. b) Width increase between the 2012-13 time interval (black circles) and 2013-15 time interval (red crosses) presented in function of depth. c) histograms in 2° classes of breakout width changes for the 2012-13 interval (black) and 2013-15 interval (red)

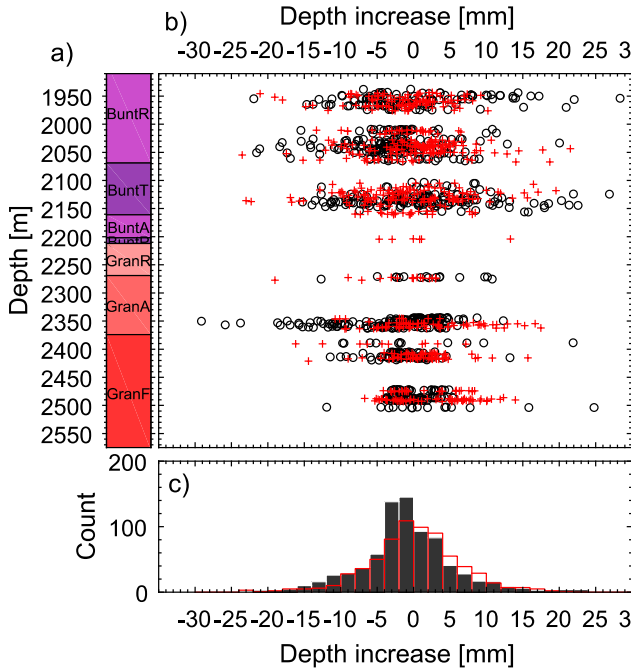

Fig. 6. Evolution of breakout depth in GRT-1 borehole. 1) Simplified lithologies along GRT1 borehole. b) Depth increase between the 2012-13 time interval (black circles) and 2013-15 time interval (red crosses) presented in function of depth. c) histograms in 2 mm classes of breakout with changes for the 2012-13 interval (black) and 2013-15 interval (red)

2012, a total breakout length of 404 m is observed and this increases to 504 m in 2013 and then remains stable in 2015 with a length of 506 m.

There is no clear evolution of DITFs along the GRT-1 well despite the hydraulic and thermal stimulation preformed between 2012 and 2013.

The increase of breakout width is presented in Fig. 5. When comparing 2012 and 2013 data, 73% of the change of width is within a -10° / +10° interval, i.e. within our measurement uncertainty. This means for these breakouts that no change of width can be highlighted. However, for 27 % of our data, a width increase larger than 10° is observed, and for these breakouts widening is undisputable. Very little changes are observed between the 2013 and 2015 with the vast majority of the measured changes remains below our uncertainty level of +/- 10°.

The evolution of breakout depth is more delicate to track because of signal loss artefact. In our analysis, we have been filtering out all obvious incorrect depth measurements related to time out artefact. The width evolution data are presented in Fig. 6. For both time interval (2012-13 and 2013-15), our breakout depth change data are symmetrically distributed about 0 mm changes and span a variability of about +/- 15 mm. We interpret this as an indication that if any deepening occurred, it remained within our uncertainty level and cannot be highlighted with our data.

5. DISCUSSIONS

The analysis presented above show that breakout geometry evolves with time. With our data, we were able to highlight without doubt a development of breakouts along the well: section of the well without breakouts in 2012 present breakouts in 2013 and 2015. Our data do not allow to precise the timing of these developments. The 2012 data was collected four days after drilling completion at a time during which the drilling induced temperature perturbation is still present. The next data set has been collected one year later and hydraulic, thermal and chemical stimulation took place in the meantime. Thus we cannot tell if the observed changes took place during the equilibration of borehole conditions directly following drilling or during the stimulations operations. No changes are observed in terms of drilling induced tension fractures: this suggests that the tensile hoop stress induced by cooling and borehole pressurization during stimulation were less intense than the one induced during drilling. The development of breakouts took place essentially in the sedimentary cover. This can be explained by the lower strength of the sediments and thus conditions closer to failure in the sedimentary section.

The study of breakout width and breakout depth allows highlighting some widening of the breakouts while deepening remained within the uncertainly level of our

measurements. These results contradict the usual assumption that breakouts typically deepen but do not widen with time. However, these results must be considered cautiously. Our analysis of breakouts depth is limited by the fact that signal loss artefact prevents sometime an accurate analysis of borehole radius and it is not always possible to estimate breakout depth reliably. Thus, we cannot absolutely exclude that breakout did not deepen. Our analyses are more conclusive concerning breakouts width, although we recognize that our breakout width evaluation is also affected by uncertainty. Indeed, the determination of the position of the border of the breakouts – from which the breakout width is computed – is not always obvious because the deviation from the nominal cylindrical borehole geometry is transitional. We mitigated this difficulty by determining the breakout shape on all datasets simultaneously to insure a consistent determination.

The impact of breakout widening on stress estimation can be evaluated considering the relation from (Barton et al. 1988) expressing SHmax in function of breakout width and other geomechanical parameters:

$$SHmax = \frac{UCS+p_p+P_w-Shmin\left(1-2\cos(2\theta_b)\right)}{1+2\cos(2\theta_b)} \qquad (3)$$

We consider typical values representative of our observations in the GRT-1 borehole. Let us assume an initial breakout width ($2\theta_b$) of 50° widening to 75° (25° of widening). We take the uniaxial compressive strength of the rock UCS = 120 MPa. We also assume a hydrostatic pore pressure and wellbore pressure at 2.5 km depth Pp = Pw = 24 MPa. The vertical stress (*Sv*) is assumed to be lithostatic with a magnitude of 64 MPa at 2.5 km (density = 2.6). The minimum horizontal stress magnitude is taken from the estimate at the neighboring site of Soultz-sous-Forêts and is equal to 0.54·*Sv*, i.e. *Shmin* = 35 MPa. According to Eq. 3, the *SHmax* estimate will increase from 78 to 100 MPa. This seems to be a significant change, but this is in fact not such a drastic difference considering the uncertainty in other parameters, particularly the strength parameters. Indeed, the uncertainty on the choice of the appropriate failure criteria and the associated strength parameters will imply uncertainties that are much larger than this range (Valley and Evans 2015). This difference will also reduce if the thermal stresses are considered. The cooling induced by drilling dissipates with time as breakouts widen accounting for part or all the difference in the stress estimate. Temperature logs at Rittershoffen suggest a cooling at the end of drilling of about 30 to 35°C. Assuming a thermal coefficient of linear thermal expansion $\alpha = 8\cdot10^{-6}$ K^{-1}, a Young modulus of 54 GPa and a Poisson's ration of 0.25, the thermal hoop stress due to cooling given by (Stephens and Voight 1982):

$$\sigma_{\Delta T} = \frac{\alpha E \Delta T}{1-\nu} \qquad (4)$$

will be equal for our parameters to -17 to -20 MPa (negative sign for tension). This explains a large portion of the observed difference, although the assumptions here are very simplistic with a purely linear elastic model without accounting for progressive failure mechanisms. Additional work to better constraint the thermal history of the well and the thermal stress evolution is on-going.

6. CONCLUSIONS

The repeated logging of the geothermal well GRT-1 in Rittershoffen (France) gives a unique opportunity to study borehole breakout evolution with time. Our analysis lead to the following conclusions:

- **(i)** Our data provides in-situ observations of breakout evolution with time;
- **(ii)** The length of breakout extends. Breakout widening is also observed but breakout deepening was not observed, within the limit of the uncertainty of our analysis. This contradict the common assumption that breakouts do not widen but only deepen until the borehole reaches a new stable state;
- **(iii)** From our data, we cannot assess if the breakout evolution took place during the thermal equilibration directly following drilling completion or during the perturbation subsequently induced by reservoir stimulation;
- **(iv)** The consequences of the breakout evolution for stress characterization are significant and add up to other important uncertainties like the estimation of strength parameters.

More insight in the observed breakout evolution can be gained by a detailed stress analysis in the reservoir and at the borehole wall, including the estimation of cooling profile and thermal stresses. This is the subject of on-going analyses.

ACKNOWLEDGMENTS

The authors are grateful to ES-Géothermie for giving access to the ECOGI datasets.

REFERENCES

Barton C, Zoback M, Burns K (1988) In-situ stress orientation and magnitude at the Fenton geothermal site, New Mexico, determined from wellbore breakouts. Geophys Res Lett 15:467–470

Baujard C, Genter A, Dalmais E, et al (2017) Hydrothermal characterization of wells GRT-1 and GRT-2 in Rittershoffen, France: Implications on the understanding of natural flow systems in the rhine

graben. Geothermics 65:255–268. doi: 10.1016/j.geothermics.2016.11.001

Cuenot N, Charléty J, Dorbath L, Haessler H (2006) Faulting mechanisms and stress regime at the European HDR site of Soultz-sous-Forêts, France. Geothermics 35:561–575. doi: 10.1016/j.geothermics.2006.11.007

Duringer P (2013) Forage de Rittershoffen GRT-1. Coupe stratigraphique et description des cuttings. University of Strasbourg EOST-CNRS - for ECOGI

Genter A, Evans KF, Cuenot N, et al (2010) Contribution of the exploration of deep crystalline fractured reservoir of Soultz to the knowledge of enhanced geothermal systems (EGS). Comptes Rendus Geosci 342:502–516. doi: 10.1016/j.crte.2010.01.006

Lengliné O, Boubacar M, Schmittbuhl J (2017) Seismicity related to the hydraulic stimulation of GRT1, Rittershoffen, France. Geophys J Int 208:1704–1715. doi: 10.1093/gji/ggw490

Lofts JC, Bourke LT (1999) The recognition of artefacts from acoustic and resistivity borehole imaging devices. Geol Soc Lond Spec Publ 159:59–76. doi: 10.1144/gsl.sp.1999.159.01.03

Manning CE, Ingebritsen SE (1999) Permeability of the continental crust: Implications of geothermal data and metamorphic systems. Rev Geophys 37:127–150. doi: 10.1029/1998RG900002

Schmitt DR, Currie CA, Zhang L (2012) Crustal stress determination from boreholes and rock cores: Fundamental principles. Tectonophysics 580:1–26. doi: 10.1016/j.tecto.2012.08.029

Stephens G, Voight B (1982) Hydraulic fracturing theory for conditions of thermal stress. Int J Rock Mech Min Sci Geomech Abstr 19:279–284. doi: 10.1016/0148-9062(82)91364-X

Teza D, Baumgärtner J, Gandy T (2013) Hydraulic stimulation experiment and tests in GRT-1. Bestec report for ECOGI

Valley B (2007) The relation between natural fracturing and stress heterogeneities in deep-seated crystalline rocks at Soultz-sous-Forêts (France). PhD thesis, Eidgenössische Technische Hochschule ETH Zürich, Nr. 17385

Valley B, Evans K (2015) Estimation of the stress magnitudes in Basel Enhanced Geothermal System. In: Proceedings of the world geothermal congress 2015

Zoback M, Barton C, Brudy M, et al (2003) Determination of stress orientation and magnitude in deep wells. Int J Rock Mech Min Sci 40:1049–1076